Photoemission, near-edge x-ray-absorption spectroscopy, and low-energy electron-diffraction study of C_{60} on Au(111) surfaces

C.-T. Tzeng
Institute of Electro-Optical Engineering, National Chiao-Tung University, Hsinchu, Taiwan, Republic of China

W.-S. Lo and J.-Y. Yuh
Synchrotron Radiation Research Center, Hsinchu, Taiwan, Republic of China

R.-Y. Chu
Department of Physics, National Tsing-Hua University, Hsinchu, Taiwan, Republic of China

K.-D. Tsuei*
Synchrotron Radiation Research Center, Hsinchu, Taiwan, Republic of China
and Department of Physics, National Tsing-Hua University, Hsinchu, Taiwan, Republic of China
(Received 10 June 1999)

The geometric and electronic structures of C_{60} adsorption on Au(111) surfaces have been studied by low-energy electron diffraction (LEED), angle-resolved photoemission, and near-edge x-ray-absorption spectroscopy. An irreversible structural transition of the C_{60} overlayer on Au(111) was observed by LEED upon successive annealing. These structures are 38×38 ''in phase,'' $R14°$ and $(2\sqrt{3}\times2\sqrt{3})R30°$, with the latter phase predominating after annealing to 350 °C. Valence-band photoemission spectra reveals a state right below the Fermi level for an annealed, ordered monolayer. This peak disperses across the Fermi energy that indicates the C_{60} overlayer becomes metallic. Its intensity shows a resonance that primarily follows the behavior of highest occupied molecular orbitals, identified unambiguously as lowest unoccupied molecular orbitals (LUMO's) filled by charge transfer from the substrate. An asymmetric distribution of LUMO charge is observed. The thermal-desorption energy of the monolayer is estimated from annealing experiments to be 1.9 eV, which is 0.5 eV larger than the desorption energy from multilayers. Comparison with available spectroscopic data indicates that interaction of C_{60} with Au(111) is slightly weaker than with Au(110), and much weaker than with Cu(111). The amount of charge transfer estimated from photoemission is 0.8 electrons per C_{60} molecule on Au(111), compared to 1.6 electrons on Cu(111). We argue that charge transfer is determined by the bulk *sp* density of states at the Fermi energy scaled by the size of the C_{60} molecule, and also modified by a clean surface electronic structure, and that charge transfer is the dominant interaction in these systems.

I. INTRODUCTION

The interaction of C_{60} with metal surfaces, or the nature of their chemical bonding, has recently attracted much interest.[1–25] One reason for this is the discovery of the superconductivity of alkali-doped compounds.[26,27] In these compounds it has been proved that there exists charge transfer from alkali atoms to the unoccupied molecular orbitals of C_{60}. The most direct evidence of this is the gradual filling of the lowest unoccupied molecular orbital (LUMO) observed in a combined study of photoemission and inverse photoemission. In this study a peak of the density of states emerges right below the Fermi level in photoemission, at the expense of the disappearance of unoccupied states detected by inverse photoemission.[28] The amount of charge transfer is closely related to transport properties. For example, for the potassium fluoride K_xC_{60}, the compound $x=3$ is metallic and shows superconductivity below 24 K,[26,27] while other compounds are insulators. For systems of C_{60} adsorption on metal surfaces, it is often concluded that charge transfer also occurs from metal substrate to the molecules. A charge-transfer peak has been observed by photoemission in Ag(111),[11–13] Cu(111),[10] and Cu and Ag films,[3,4] but not in Au(110).[6] The amount of charge transfer on a metal surface has been measured indirectly by a shift of C_{60} vibrational energies by high-resolution electron-energy-loss spectroscopy (HREELS) in Au(110),[5] Ni(110),[16] and Cu(111),[29] or by shift of carbon core-level absorption spectra using EELS in Au(110),[5] and using new-edge x-ray-absorption spectroscopy (NEXAFS) in Cu(111),[10] compared to shift of alkali-doped compounds where the amount is known,[30] or by a direct comparison of relative photoemission intensities in Ag(111) (Ref. 12) and Cu(111).[10] In cases of Al(111) (Refs. 23 and 25) and Pt(111),[17] where no sign of charge-transfer peaks could be observed, or the opposite direction of the shift in NEXAFS or HREELS was measured, covalent bonding was instead proposed to explain the experimental results. The C_{60} overlayer structures have also been studied by scanning tunneling microscopy (STM) on a variety of metal surfaces.[31–38] Information about charge transfer can be deduced.[31] In this regard the character of the overlayer-substrate interaction is crucial to understanding the initial growth of films.[39]

For a number of reasons we choose Au(111) as the substrate to study the electronic and geometric structures of C_{60} overlayers. First, there exists a bulk-projected band gap around the Fermi level at the surface Brillouin-zone center in Au(111), similar to these for Cu(111) and Ag(111). A charge-transfer peak has been observed in photoemission in the latter two systems due to the low background emission

from the substrate.[10–12] Second, detailed studies on the electronic structures of C_{60} on Cu(111) (Ref. 10) and Au(110) (Ref. 6) have been carried out, and the amount of charge transfer on Ag(111) (Ref. 12) and polycrystalline surfaces of all three noble metals (Ref. 4) has also been reported. A study on Au(111) would enable us to compare the interaction of C_{60} on the same surfaces but on different noble metals, and on different surfaces but the same metal, and compare polycrystalline surfaces with single-crystal surfaces. Third, a STM study reported an in-phase incommensurate structure and a commensurate $(2\sqrt{3}\times 2\sqrt{3})R30°$ structure in the monolayer region, but no LEED patterns could be observed,[32] while another x-ray-diffraction study of thick epitaxial films found a third structure of $R\pm 14°$ that could become dominant, depending on the growth temperature.[40]

In this paper we report a LEED observation of all three structures upon annealing, probing of the electronic structure using angle-resolved valence-band photoemission, carbon core-level photoemission, and NEXAFS, and a thermal-desorption measurement. We found that the interaction of C_{60} with Au(111) is still chemisorption, but the weakest among the metal surfaces studied so far. The amount of charge transfer is measured and, by comparing with existing studies on noble-metal surfaces, we conclude that charge transfer from substrate *sp* electrons dominates the interaction in these systems.

II. EXPERIMENT

The experiment was carried out at the Synchrotron Radiation Research Center in Hsinchu, Taiwan using low-energy spherical grating monochromator and high-energy spherical grating monochromator beamlines. Photoemission was done in an ultrahigh-vacuum chamber equipped with LEED, and a 200-mm-radius hemispherical analyzer aligned with a fixed 50° angle to the incident photon beam with a base pressure of 1×10^{-10} torr. The angular acceptance can be controlled by an adjustable aperture and it was $\pm 1°$ for angle-resolved valence-band photoemission measurements. Photon energies from 22 to 60 eV were used. The overall energy resolution was 0.1 eV at 22 eV and 0.14 eV at 60 eV. For C 1*s* core-level photoemission, an acceptance angle of $\pm 8°$ was used, and a photon energy of 330 eV was chosen to maximize the intensity. The overall energy resolution was better than 0.4 eV. For the C 1*s* NEXAFS measurement, total electron yield detection was used, and the signal was normalized to the photocurrent from a freshly evaporated Au mesh placed in front of the sample. The incident angle was 50° to the surface normal. The crystal was cleaned by cycles of 1.5-keV Ar-ion sputtering and annealing. The C_{60} evaporator has been described previously.[10] Evaporation and measurements were done at room temperature (RT). The C_{60} monolayer could be prepared by annealing a sample to 300 °C to desorb multilayers. The unannealed ML film was calibrated by core-level intensity, thickness monitor reading, and the attenuation of surface state of Au(111).

III. RESULTS AND DISCUSSION

A. Low-energy electron diffraction

We performed LEED measurements of C_{60} overlayers on a Au(111) surface to study the evolution of structural transformation as a function of annealing temperature. A LEED pattern at 10-eV incident electron energy for a film of about 4 ML of C_{60} deposited at RT is shown in Fig. 1(a). We found that the LEED pattern of the C_{60} overlayers could only be observed when the kinetic energy of the incident electron beam was less than 30 eV. A higher incident electron energy caused a higher background and, as a result, the LEED spots became difficult to see. The observed 18 spots can be classified as three groups of hexagons with axes either aligned or with an approximately $\pm 14°$ azimuthal rotation with respect to the clean substrate LEED pattern, displayed in Fig. 1(d). The former phase is called an ''in-phase'' structure that consists of a 38×38 substrate unit cell containing 11×11 C_{60} molecules.[32] The rotational angle of the $R14°$ structure may vary slightly, as has been examined by x-ray diffraction.[40] The intensity modulation of the in-phase and $R14°$ structures are similar in the range of 7–25-eV electron energies, indicating many domains of epitaxially grown multilayers, which suggests that the LEED patterns observed also correspond to the structure of the first monolayer. The intermolecular spacing of C_{60} is estimated to be about 10 Å, deduced by comparing C_{60} LEED spots with the substrate LEED pattern.

Figure 1(b) shows the LEED pattern of the same film after annealing to 200 °C and back to RT using 8-eV incident electrons. A structure appears in this LEED pattern with a rotated angle at 30° compared with the in-phase structure, and is identified as a $(2\sqrt{3}\times 2\sqrt{3})R30°$ structure.[32] Unlike the in-phase and $R14°$ structures, C_{60} in this $(2\sqrt{3}\times 2\sqrt{3})R30°$ structure forms a commensurate overlayer on the unreconstructed Au(111) surface. It is believed to be a thermodynamically favored structure on Au(111).[32] We note that the intensity of the in-phase spots decreases relative to the $R14°$ structure, and the new $(2\sqrt{3}\times 2\sqrt{3})R30°$ spots are as intense as the $R14°$ spots.

The LEED pattern using 19-eV electrons after an annealing to 350 °C is displayed in Fig. 1(c). Only 1 ML remained on the surface. Although the LEED spots of the three observed structures show different intensity modulations at different incident electron energies due to the substrate effect, we can still identify $(2\sqrt{3}\times 2\sqrt{3})R30°$ as the most dominant structure. The other two structures disappeared almost completely after annealing to 420 °C. Further annealing causes a weakening of the intensity of the $(2\sqrt{3}\times 2\sqrt{3})R30°$ LEED spots and a simultaneous recovery of the substrate pattern, indicating desorption of C_{60} molecules. Final annealing to 480 °C results in a clear substrate pattern only. In summary, our LEED study indicates that the C_{60} molecules form in-phase and $R14°$ structures on Au(111) surfaces at RT. Annealing transforms the in-phase structure to $R14°$ structure, and then to a $(2\sqrt{3}\times 2\sqrt{3})R30°$ structure.

Our LEED observation is in general agreement with the x-ray-diffraction study on thick films grown between 130 and 290 °C.[40] In this study the $(2\sqrt{3}\times 2\sqrt{3})R30°$ structure appeared only as a minor component and the in-phase and $R14°$ structures dominate at low and high temperatures, respectively. On the other hand, we observed a large fraction of $R14°$ even at RT. This can be attributed to our much lower evaporation rate ($\sim$0.05 ML/min) than that used ($\sim$22 ML/min) in Ref. 40. The C_{60} molecules would have enough time to diffuse to the more stable $R14°$ structure even at RT

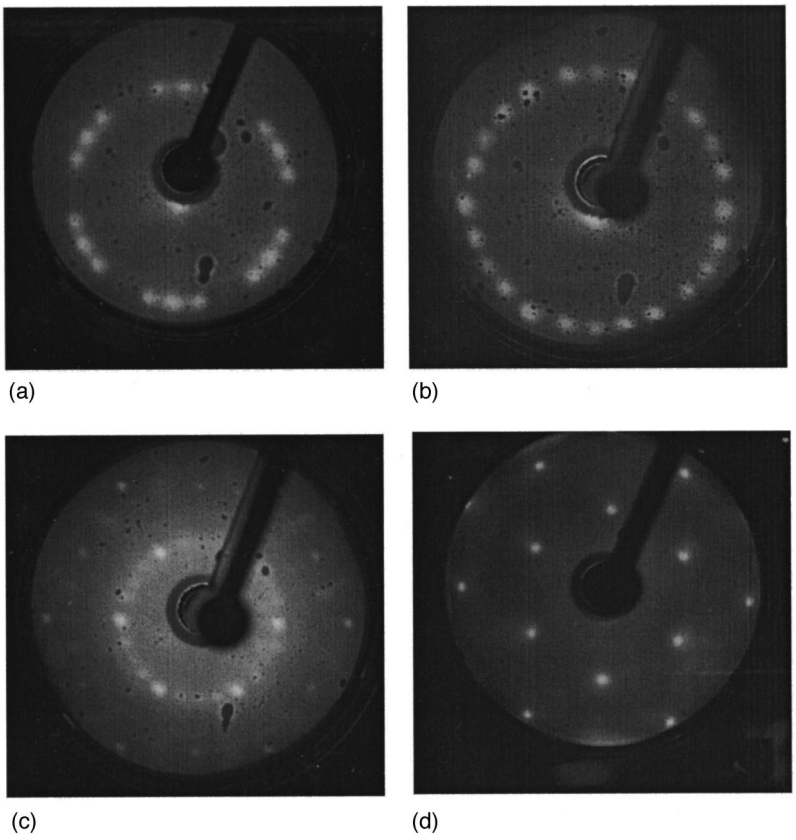

FIG. 1. LEED patterns (a) of a 4-ML C_{60} film on Au(111) deposited at RT at 10-eV electron energy; (b) after annealing to 200 °C at 8 eV; (c) after annealing to 350 °C at 19 eV, at which time only 1 ML remained on the surface; and (d) of a clean Au(111) surface at 150 eV.

at a low evaporation rate. It is not clear why the $R14°$ structure was not observed in the STM study.[32] It is not necessary to stabilize this structure by multilayers because it still exists after annealing to 350 °C, at which only one ML remains.

B. Angle-resolved valence-band photoemission

The normal-emission spectra for a clean Au(111) surface, a 1-ML C_{60}-covered surface, and a 3-ML film are presented in Figs. 2(a), 2(b), and 2(c), respectively. The peak group between 2- and 7-eV binding energies in the clean spectrum is due to the Au *d* band. Two strong peaks at 0.3 ($S1$) and 7.7 eV ($S2$) are surface states in the bulk-projected band gaps at the surface Brillouin-zone center.[41] For the 3-ML C_{60}-covered surface, the Au features are buried completely, and what can be observed are only the molecular orbitals of C_{60}. We label the first four features by numbers as indicated. Peaks 1 and 2 stand for the highest occupied molecular orbital (HOMO) and HOMO-1, and they are π derived with an angular momentum l equaling 5 and 4, respectively.[42] Features 3 and 4 are mixtures of π and σ orbitals.[43] For the 1-ML film the C_{60} MO's are barely discernible because of direct overlap and hybridization with substrate valence bands. One can still observe a shift of the MO's towards the Fermi level, and identify the small peak at 1.7 eV as HOMO derived. Both surface states attenuate completely. Further, it can be seen that a new peak appears right below the Fermi energy.

In Fig. 3 we present details of the valence-band structure near the Fermi energy for several surface conditions. Figure 3(a) is for a clean Au(111) surface, and the peak at 0.3 eV is the *sp*-derived surface state $S1$, as stated above. The asymmetric line shape toward the Fermi energy is due to strong positive dispersion and our finite angular resolution. Figures 3(b) and 3(c) show spectra of C_{60} thin films about 1 and 1.2 ML, respectively. It can be seen that the surface state intensity is very attenuated, while some new peak emerges right below the Fermi energy. After annealing the 1.2-ML film to 200 °C, which is not high enough to desorb the second layer,

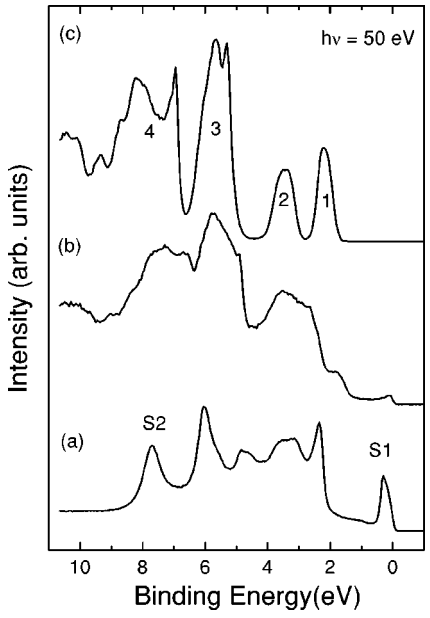

FIG. 2. Angle-resolved valence-band photoemission spectra from (a) Au(111), (b) annealed 1-ML C_{60} on Au(111), and (c) a 3-ML C_{60} thin film. Features 1 and 2 stand for HOMO and HOMO-1, respectively, for the 3-ML film.

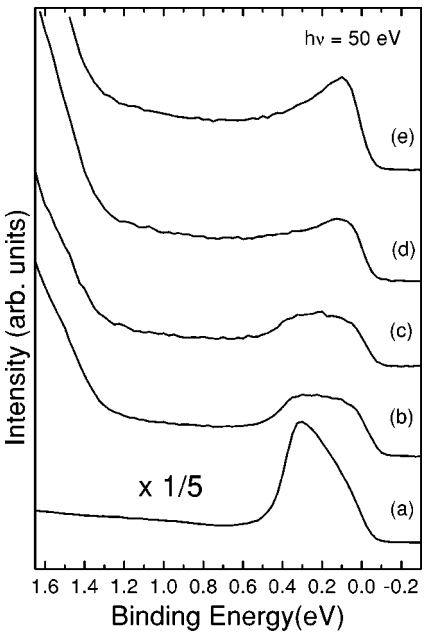

FIG. 3. Valence photoemission spectra near the Fermi energy (a) for Au(111); (b) for 1-ML C_{60} on Au(111); (c) for 1.2-ML C_{60} on Au(111); (d) after annealing to 200 °C, and (e) after annealing to 300 °C, at which time only 1 ML remained on the surface. All spectra have been normalized to sample currents and plotted on scale except (a), where the intensity has been multiplied by a factor of 1/5.

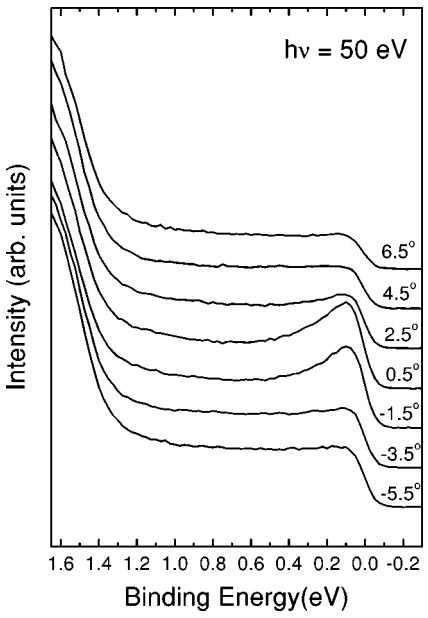

FIG. 4. Valence photoemission spectra from an annealed 1-ML C_{60} thin film at different emission angles.

the surface state disappears completely, leaving only the peak at 0.1-eV binding energy, as shown in Fig. 3(d). The second layer C_{60} has diffused down to fill the vacant region of the first layer. This indicates that the first-layer–substrate interaction is stronger than the first-layer–second-layer interaction, which is due to the van der Waals force. Further annealing to 300 °C to desorb the second layer causes the new peak intensity to grow drastically, as revealed in Fig. 3(e). Although the film annealed to 200 °C might still contain second-layer C_{60}, these extra C_{60} molecules would only attenuate the emission intensity uniformly above the HOMO, or 1.7 eV.[10] Therefore, the peak intensity of the 300 °C annealed film is higher than the intensity of the 200 °C annealed film, which reflects the real electronic structure change of the first adsorbed monolayer. From LEED study it is observed that the RT monolayer structure is mixed with in-phase and $R14°$ structure, in which the C_{60} molecules occupy many sites; further annealing causes the replacement by the commensurate, single-site $(2\sqrt{3}\times 2\sqrt{3})R30°$ structure with larger domain size. Thus the growing in intensity of the 0.1-eV peak is closely related to the long-range ordering of the C_{60} overlayer and commensurability with the substrate, similar to the case of C_{60} on Cu(111) surfaces.[10]

The angular dependence of the emission spectra measured along $\overline{\Gamma}\,\overline{M}$ of the $(2\sqrt{3}\times 2\sqrt{3})R30°$ structure from the 300 °C annealed monolayer film near the Fermi energy is displayed in Fig. 4. The zone boundary $\overline{M}$ corresponds to a polar angle of 5.2°. It is clearly seen that the 0.1-eV peak appears only in a small range around the normal-emission geometry, and quickly disappears away from normal emission presumably due to dispersion across the Fermi level. That we could not measure a finite dispersion is partly due to limited resolution both in the energy of 0.1 eV and the angle of $\pm 1°$ in the measurement. We note that this peak in the normal-emission spectrum has a low-energy tail extending down to about 0.6 eV, where it merges into a background, while the spectrum closest to the zone boundary M at $-5.5°$ contains only a Fermi-level step with a flat background. We then subtract all other spectra by this background spectrum aligned at 0.6 eV. The resulting difference spectra show that the tail of the peak moves toward the Fermi energy as the polar angles increase, indicating upward dispersion. We estimate the Fermi-level crossing from the disappearance of the peak intensity, and calculate the occupied charge associated with this, assuming only one band to be about 0.8 electrons per C_{60} molecule with an uncertainty of ± 0.2 electrons. This is to be compared to 1.6 electrons per C_{60} molecule for C_{60} on Cu(111).[44,29] We thus associate this band as one of the three LUMO (t_{1u})-derived orbitals, which transforms like a p_z orbital. The Fermi-level crossing is direct evidence that this C_{60} monolayer becomes metallic.

In order to further confirm that the 0.1-eV peak is due to charge transfer to the LUMO, we measured the normal-emission valence-band spectra including the HOMO of a 1-ML annealed film at various photon energies shown in Fig. 5. It can be seen that the HOMO peak resonates in intensity at about 44 eV while the 0.1-eV peak reaches its highest intensity around a similar energy. This cross-sectional final-state resonance behavior has been studied on thick C_{60} films,[43] single crystals,[45] and on the gas phase.[46] Recently these resonances were explained semiquantitatively in simple models in which the final states are spherical waves with a radial wave function in the form of spherical Bessel functions $j_{l_f}(kr)$.[47] The initial-state wave function is localized mainly at $r\sim R$, where R is the radius of the C_{60} molecule. Dipole selection rule and final-state wave function arguments further restrict $j_{l_{i-1}}$ as the major component. Thus cross-section minima occur when $j_{l_{i-1}}(kR)=0$. The bottom two curves in Fig. 6 plot the intensity variation for a thick

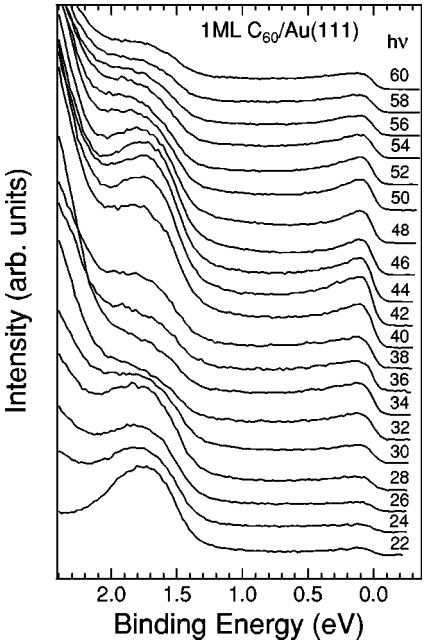

FIG. 5. Photon energy dependence of valence photoemission spectra for a 1-ML C_{60} thin film. These spectra have been normalized to sample currents.

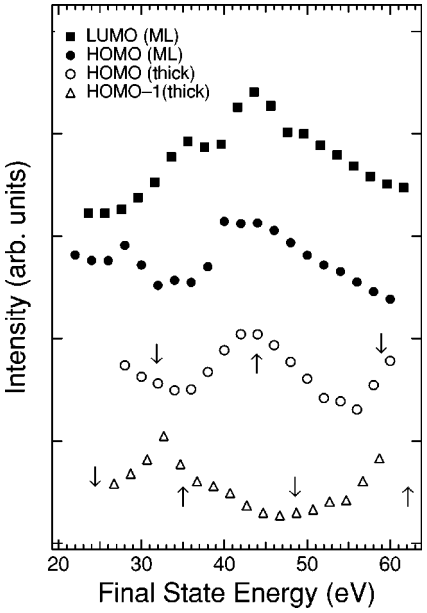

FIG. 6. Photoemission peak intensities as a function of final-state energy relative to the HOMO binding energy for a thick film, (open symbols) and a ML film (closed symbols), from Fig. 5. Intensities for a thick film have been normalized to feature 4 shown in Fig. 1 in each spectrum. All symbols are integrated peak areas except the LUMO of 1 ML (closed squares), where the peak heights are plotted. The baselines of these curves are shifted for clarity.

film as a function of final-state energy of HOMO-1 ($l=4$, open triangles) and the HOMO ($l=5$, open circles), respectively, normalized to the integrated area of feature 4 in Fig. 2 to cancel the effect of the monotonic decrease of the cross section as the photon energy increases.[43] This final-state energy is referenced to the HOMO, and has to be adjusted to the measured binding-energy difference, which is 1.3 eV for HOMO-1. The down and up arrows indicate the zeros and maxima, respectively, of $|j_3(kR)|$ and $|j_4(kR)|$ using parameters from Ref. 47. The agreement between this simple model and the experimental data is quite good. For the 1-ML film, the HOMO intensity is obtained by subtracting the high-binding-energy tail from the substrate *d*-band and HOMO-1, without normalizing to the corresponding feature 4 because of an overlap with substrate bands. It is seen in Fig. 6 that the HOMO resonance in a 1-ML film still follows thick-film behavior. For the 0.1-eV peak at 1 ML, the peak heights are plotted. The measured binding-energy difference 1.6 eV is used to convert to final-state energy. It is further seen that the maximum of the 0.1-eV peak at 43 eV matches that of the HOMO very well. This is a strong indication that the 0.1-eV peak has primarily an angular momentum $l=5$, which is exactly the same as the LUMO. It is also noted that the minimum is not quite reproduced, and a shoulder appears at about 35 eV, which is close to the resonance maximum of an $l=4$ initial state like HOMO-1. The deviation from spherical character of the LUMO is mainly due to the fact that the transferred charge from the substrate is not uniformly distributed around the molecule, and thus mixed with other angular components.

We comment at the end of this section that a scanning tunneling spectroscopy (STS) study reported a gap of less than 0.2 eV (Ref. 33) while our valence-band photoemission data shows no gap at all. Similarly, a peak right below the Fermi energy in C_{60}/Ag(110) was observed in a photoemission measurement (Ref. 15), while STS reveals a dip in the Fermi position.[34] This was interpreted as due to the different surface sensitivities of the two techniques. Photoemission probes all C atoms in the monolayer including the atoms at the interface. In contrast, STS probes just the actual top C atoms.[15] It can be understood that charge transfer to the LUMO has more weight on the C atoms closer to the interface than those on top. This explanation agrees with our resonance measurement. Finally it is noted here that an anisotropy in the remaining unoccupied part of the LUMO was recently observed in C 1*s* NEXAFS of C_{60}/Al.[24]

C. Core-level photoemission and NEXAFS

Figures 7(a) and 7(b) show the C 1*s* core-level photoemission spectra for a thick film and a 1-ML film, respectively. It is seen that the width of the peak from a 1-ML film is much broader than that from a thick film. This reflects the strong interaction nature at the interface, similar to other C_{60} on metal systems. Moreover, the monolayer line shape is slightly asymmetric toward higher binding energy, consistent with the conclusion of being metallic with a small amount of charge transfer from the angle-resolved valence-band photoemission study, in contrast to C_{60} on Cu(111) where a larger charge transfer and a very asymmetric C core-level line shape is observed. In addition, the satellite structure seen in thick-film spectra seems weakened or widened considerably. The discussion of these structures has appeared in a number of papers, and will not be repeated here.[48,49,10] We just note that the first satellite, which corresponds to a HOMO to LUMO transition, is still noticeable while completely washed out in the case of Cu(111),[10] and barely discernible in Au(110).[6] Further, the second-layer core-level peak is

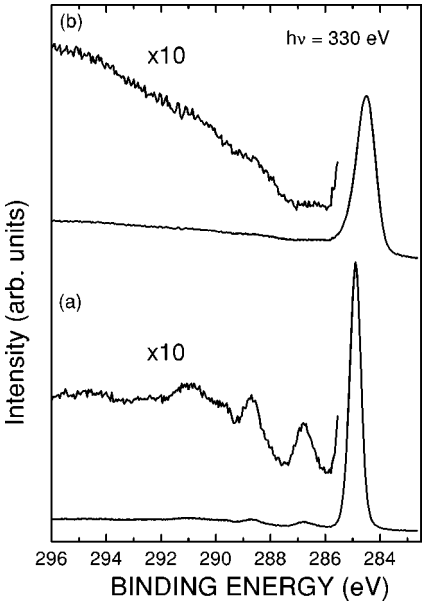

FIG. 7. C 1*s* core-level spectra for (a) a thick C_{60} film, and (b) a 1-ML film on Au(111), scaled to have the same peak areas. Intensities in the satellite regions have been multiplied by a factor of 10 as shown.

only 0.25 eV lower than that of the 1-ML film at 284.5-eV binding energy (not shown), and the shift is much smaller than 0.6 eV of Cu(111),[10] while comparable to 0.3 eV of Au(110).[6]

A carbon 1*s* NEXAFS measurement was performed to probe the conduction-band structure, as shown in Figs. 8(a) and 8(b) for a 4-ML film and an annealed 1-ML film, respectively. It is surprising to observe that the first four π^*-derived peaks of the 1-ML film, labeled 1–4 for the 4-ML spectrum, are not greatly deformed. The most notable feature from the comparison of 1- and 4-ML films is that LUMO+1, or peak 2 in C_{60}/Au(111) is only broadened, while it completely disappears in all other studied C_{60}/metal systems.[6,10,23,25] A closer examination shows that LUMO +1 attenuates more than LUMO and LUMO+2 (peaks 1

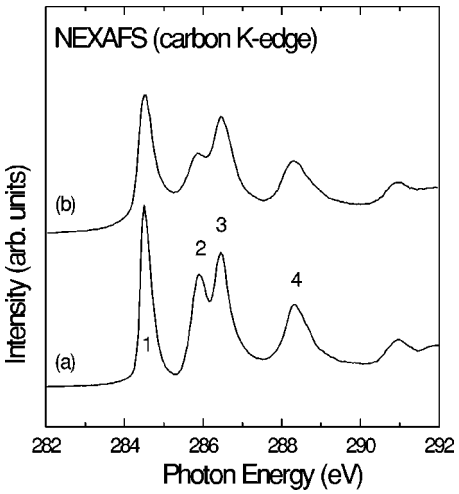

FIG. 8. C 1*s* NEXAFS spectra from (a) solid C_{60}, and (b) 1-ML C_{60} on Au(111). The first four peaks are labeled in successive order as LUMO, LUMO+1, LUMO+2, and LUMO+3.

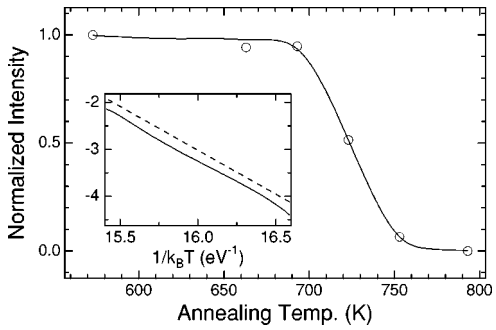

FIG. 9. Normalized C 1*s* core-level peak intensities as a functions of annealing temperature, shown as open circles. The solid line represents a smoothed interpolation between data points. The inset shows a first-order logarithm plot of the same solid line according to Eq. (2) in the temperature range of desorption, and the dashed line is a linear fit to the solid curve with a slope of 1.87 eV, and is shifted for clarity.

and 3). This behavior is in agreement with the theoretical calculation that LUMO+1 has a larger dispersion due to a larger overlap with neighboring molecules.[50] As a result it becomes easier to perturb by substrate states. The survival of the LUMO+1 peak only in NEXAFS of C_{60}/Au(111) indicates that the conduction band is only slightly disturbed, and that the interaction of C_{60} with Au(111) is the weakest among the metal systems so far studied. This weak interaction also reflects in the coincidence of LUMO peak energy with C 1*s* core-level binding energy, as in Au(110),[6] in sharp contrast to Cu(111), where the core-level binding energy corresponds to a clear absorption threshold at a lower photon energy.[10]

D. Thermal desorption

We performed thermal-desorption measurement in order to obtain the strength of C_{60}-metal surface interaction. Starting from a completely covered ML film by annealing to 300 °C, valence-band photoemission spectra taken after subsequent annealing to higher temperatures reveal that C_{60} simply desorbs from the Au(111) surface and does not decompose into fragments, consistent with LEED studies. The carbon 1*s* core-level intensity measured at RT after annealing provides a quantitative determination of how much C_{60} is left on the surface. The results, normalized to the intensity from a complete monolayer, are plotted in Fig. 9 as open circles. The solid curve is a smoothed interpolation between the data points. It is seen that C_{60} desorbs almost completely by annealing to 750 K. This temperature is the lowest among all metal surfaces studied so far,[25] consistent with the conclusion based on the NEXAFS line shape described in Sec. III C, that the interaction of C_{60} with Au(111) is the weakest. The desorption energy is thus estimated in the following way. According to the Polanyi-Wigner model, the desorption rate can be expressed as[51]

$$-dN/dt = k_m N^m \exp(-E_d/k_B T), \tag{1}$$

where N is the C_{60} coverage, k_m is a frequency prefactor, m is the order of desorption process, and E_d is the activation energy of desorption. If the desorption process is only related

to individual molecules and mutual interaction is not important, $m=1$, and the desorption is first order. However, from a submonolayer study by STM, C_{60} tends to form islands at RT, indicating an attractive force between adsorbed molecules.[32] If the desorption is primarily from the rim of the islands, then $m=\frac{1}{2}$, and the desorption is half order. We further assume that the heating rate is constant for all annealing processes, and thus end up with two equations

$$\ln(-d\ln N/dT) = -E_d/k_BT + c \tag{2}$$

for first-order desorption, and

$$\ln(-dN^{1/2}/dT) = -E_d/k_BT + c' \tag{3}$$

for the half-order process. The inset in Fig. 9 plots the logarithms vs $1/k_BT$ for the first-order process in the temperature range of desorption. It is seen that the curve can be well fitted with a straight line with a slope of 1.87 eV (43 kcal/mole), which represents the desorption energy. Fitting to the half-order process would yield a poorer fit with a value less than 1 eV. The thermal-desorption energy measured from multilayers gives 1.4 eV.[52,53] It is unlikely that a chemisorbed C_{60} molecule would desorb from the rim of a chemisorbed monolayer island with a desorption energy smaller than that from thick C_{60} films bound by van der Waals force. Therefore, we conclude that only the first-order process is observed in our thermal-desorption measurement.

A first-order desorption can be understood from any adatom near saturation coverage. For lower coverages where C_{60} forms islands, first-order desorption would imply that the C_{60}-substrate interaction is much larger than the lateral interaction between molecules in an island, where a molecule at the rim, though with less coordination than in the center, has a similar binding energy. The lateral interaction of a C_{60} monolayer contains the band formation energy of the occupied LUMO by charge transfer, which is of the order of 0.1 eV. For a C_{60} molecule in the first layer of the (111) surface of a solid, the lateral van der Waals interaction from surrounding molecules can be estimated from Lennard-Jones potential to be 1.1 eV,[54] where a measured bulk cohesive energy of 1.5 eV is used.[55] Hence the lateral interaction cannot be neglected in the desorption of a C_{60} monolayer. Another possibility of the first-order process is that C_{60} transforms to a ''gas'' phase from a ''solid'' (island) phase before desorption. This would result in different desorption energies for different coverage regimes.[51] It is further complicated by the removal of Au(111) surface reconstruction by C_{60} adsorption.[32] These issues cannot be resolved from our limited results.

E. Work-function change

We measured the work function by performing a photoemission measurement on the secondary edge rise and the Fermi-level cutoff using He I (21.2 eV) as the photon source. The known photon energy minus the total spectrum width yields the absolute work function. The measured work function of 1-ML C_{60} on Au(111) was 4.7 eV, which is 0.6 eV *lower* than the clean surface value despite charge transfer *from the substrate to the* C_{60} *overlayer*. For C_{60}/Au(110) a 0.55-eV decrease from the clean surface value to 4.82 eV has been reported,[25] similar to our Au(111) results. A simple argument of dipole formation due to charge transfer would *increase*, instead of decrease, the work function, which is *opposite* to the observation.[9,10] Our result is similar to most other monolayer C_{60}/metal systems with final work functions close to 5 eV, whether or not the original substrate work functions are higher or lower than 5 eV.[25,10] This is explained by the fact that the chemisorbed monolayer becomes metallic, due to charge transfer from the substrate. The image plane moves from the interface to the outside of the metallic overlayer, and the interface dipole layer created by the charge transfer is screened out by the image plane. Therefore, the measured work function for a monolayer film is purely due to the metallic overlayer, and is not related to the interface.[9,10] It is interesting to note here that the work function of graphite is just 5 eV.[56] It has also been argued that the large size of a C_{60} molecule and its many possible excitation channels might render the dipole model invalid.[25] More experimental measurements and theoretical studies are needed to clarify this point.

F. Comparison of C_{60}-Au(111) interaction with Au(110) and Cu(111)

In this section we discuss a further comparison of our spectroscopic results with the existing studies on Au(110) (Ref. 6) and Cu(111),[10] as well as their overlayer structures. A C_{60} overlayer removes original reconstruction on the clean Au(111) surface, and forms three structures on an unreconstructed surface, with the commensurate, single-sited $(2\sqrt{3}\times 2\sqrt{3})R30°$ structure being the most stable structure.[32] On the other hand, C_{60} does not remove the 1×2 missing-row reconstruction of the clean Au(110) surface. It further induces multiphases of 1×2, 1×3, and 1×4 reconstructions on an overdosed, annealed monolayer.[35] The C_{60} adsorption on a reconstructed Au(110) surface should be stronger than on a (111) surface without reconstruction. This reflects the survival of the first satellite peak in C 1*s* core-level photoemission and the LUMO+1 peak in C 1*s* core absorption spectra in the case of Au(111), but these features are barely discernible in Au(110).[6] The slightly higher desorption temperature of C_{60} on Au(110) than on Au(111) is consistent with the above observation.[32,25] However, the difference cannot be large. The very asymmetric C 1*s* core-level line shape of C_{60}/Au(110) could be partly due to multiple sites, but should also receive a significant contribution from better metallic screening in that more charge transfer occurs on (110)than (111) surfaces.[5] The reason why no charge-transfer peak was observed in the photoemission study on Au(110) (Ref. 6) could be due to disorder in the overlayer, and the lack of a substrate band gap to clearly reveal the small charge transfer.

It is obvious that C_{60} interacts more strongly with Cu(111) than with Au(111) surfaces, as seen in the larger C 1*s* core-level shift and in larger changes in C core-level satellites and absorption spectra in Cu(111). For the most stable $(2\sqrt{3}\times 2\sqrt{3})R30°$ structure on Au(111), STM concludes that C_{60} adsorbs on an on-top site with a five-member ring facing

TABLE I. Measured charge transfer per C_{60} molecule on noble-metal surfaces, and some surface and bulk properties of noble metals. The total surface-state charges and total bulk sp-DOS(E_F) have been multiplied by the size of the surface unit cells. They are $(2\sqrt{3}\times 2\sqrt{3})R30°$ for Au(111) and Ag(111), and 4×4 for Cu(111).

	Au	Ag	Cu
Charge transfer from the (111) surface	0.8[a]	0.75[b]	1.6[d]
Total clean (111) surface-state charge[e]	0.42	0.23	0.67
Charge transfer from the polycrystalline surface[f]	1.0	1.7	1.8
Total sp-DOS(E_F)[g] (states/Ry/surf. unit cell)	18.7	33.2	32.6

[a]Present work.
[b]Reference 12.
[c]Reference 29.
[d]Reference 44.
[e]Reference 41.
[f]Reference 4.
[g]Reference 58.

the surface, and with a rotational disorder.[32,33] C_{60}, on the other hand, forms a 4×4 structure on Cu(111), and adsorbs on a threefold hollow site with a six-member ring facing down and an ordered orientation.[31] The rotational disorder is consistent with the weaker interaction with the substrate. Annealing experiments indicate that C_{60} desorbs and even decomposes on Cu(111) surfaces at a temperature higher than the desorption temperature on Au(111), and that offers a direct comparison of their relative interaction strength.[57] The related spectroscopic studies of C_{60} on Ag(111) are not available. An STM study observed a $(2\sqrt{3}\times 2\sqrt{3})R30°$ structure (Ref. 32), and an x-ray-diffraction experiment measured a $R14°$ phase,[40] quite similar to what happens in Au(111).

G. Charge transfer and interaction of C_{60} on noble-metal surfaces

Finally, we compare the measured charge transfer on the (111) and polycrystalline surfaces of Au, Ag, and Cu to discuss its origin. These values are listed in Table I. In the table we also include the clean (111) surface state charges,[41] and the bulk *sp* density of states (DOS) at the Fermi energy [DOS(E_F)] scaled to the size of surface unit cell for comparison.[58] It is immediately seen that the ratios between the measured charge transferred from polycrystalline surfaces and the total sp-DOS(E_F) are remarkably similar for all three noble metals. The measured charge transfer from the (111) surfaces of Au and Cu, which are slightly less than the values from polycrystalline surfaces, are also approximately proportional to total sp-DOS(E_F), but charge transfer from Ag(111) deviates greatly from this trend. The total clean (111) surface-state charges of Au and Cu are approximately half of the charges transferred to C_{60}, while that of Ag is much lower. The smaller quantity and higher binding energy than those of the (occupied) LUMO indicate that this surface state is not directly responsible for charge transfer. However, it strongly suggests that for noble metals charge transfer is determined by a bulk sp-DOS(E_F) scaled by the size of the C_{60} molecule, and also modified by a clean surface electronic structure in the case of the identical single-crystal surfaces but different metals. For different surfaces of the same metal like Au(111) and Au(110) the different spectroscopic line shapes and desorption temperatures reflect the difference in the surface electronic structure. In the above discussion we consider only *sp* electrons rather than *d* states, because the former is more delocalized to make a significant contribution to charge transfer to the C_{60} LUMO, which is originally delocalized to the whole, large molecule. We now discuss the influence of the *d* bands on the total chemical bonding. The *d* bands are all well below the Fermi energy, and their positions are quite similar for Au and Cu, with Ag slightly lower. The interaction between C_{60} and surfaces should not depend much on *d* bands compared to *sp* states, and charge transfer is the dominant interaction in these systems. We remark here that C_{60} desorbs at about the same temperature on both Ag(111) and Au(111),[32] in agreement with the fact that the amount of charge transfer is similar on these surfaces.

IV. CONCLUSIONS

We performed an extensive study of the C_{60} overlayer on Au(111) by photoemission, NEXAFS, and LEED. LEED patterns are clearly observed at low incident electron energies below 30 eV on this surface. An irreversible geometrical structural transition shows successive evolution of in-phase, $R14°$, and $(2\sqrt{3}\times 2\sqrt{3})R30°$ structures as the sample is annealed, with the latter being the most stable phase. It is found in angle-resolved photoemission that a new state forms right below the Fermi level for an annealed, ordered C_{60} monolayer. It disperses across the Fermi level, proving directly that the C_{60} overlayer is metallic. Its intensity shows a resonance in photon energy primarily following the character of the HOMO, thus can be identified unambiguously as the LUMO. The resonance also indicates aspherical distribution of the LUMO charge. This result substantiates the model of charge transfer from substrate to adsorbed C_{60} molecules. Comparison of the present C 1*s* core-level satellite intensities and NEXAFS spectra with published data indicates a slightly stronger interaction of C_{60} with the Au(110) substrate than with Au(111) but a much stronger interaction with Cu(111). Specifically the amount of charge transfer can be estimated with 0.8 electrons per C_{60} molecule on Au(111)compared to 1.6 electrons on Cu(111). We found that the amount of charge transfer to polycrystalline surfaces is determined by the sp-DOS at the Fermi energy of metal sub-strates, while it is also modified by the surface electronic structure on single-crystal surfaces. We conclude that charge transfer is the dominant term in C_{60}–noble-metal surface interaction.

ACKNOWLEDGMENTS

We thank the staff of the SRRC for their technical assistance, and A. B. Yang for in loan of a Au crystal. One of us (K.D.T.) is grateful to Y.-W. Yang and K.-J. Song for useful discussions on thermal desorption. This work was in part supported by the National Science Council of the ROC.

*Author to whom correspondence should be addressed. Electronic address: tsuei@srrc.gov.tw

[1] T. R. Ohno, Y. Chen, S. E. Harvey, G. H. Kroll, J. H. Weaver, R. E. Haufler, and R. E. Smalley, Phys. Rev. B **44**, 13 747 (1991).

[2] T. R. Ohno, Y. Chen, S. E. Harvey, G. H. Kroll, P. J. Benning, J. H. Weaver, L. P. F. Chibante, and R. E. Smalley, Phys. Rev. B **47**, 2389 (1993).

[3] S. J. Chase, W. S. Bacsa, M. G. Mitch, L. J. Philione, and J. S. Lannin, Phys. Rev. B **46**, 7873 (1992).

[4] B. W. Hoogenboom, R. Hesper, L. H. Tjeng, and G. A. Sawazky, Phys. Rev. B **57**, 11 939 (1998).

[5] S. Modesti, S. Cerasari, and P. Rudolf, Phys. Rev. Lett. **71**, 2469 (1993).

[6] A. J. Maxwell, P. A. Bruhwiler, A. Nilsson, N. Martensson, and P. Rudolf, Phys. Rev. B **49**, 10 717 (1994).

[7] M. Pedio, M. L. Grilli, C. Ottaviani, M. Capozi, C. Quaresima, P. Perfetti, P. A. Thiry, R. Caudano, and P. Rudolf, J. Electron Spectrosc. Relat. Phenom. **76**, 405 (1995).

[8] J. E. Rowe, P. Rudolf, L. H. Tjeng, R. A. Malic, G. Meigs, C. T. Chen, J. Chen, and E. W. Plummer, Int. J. Mod. Phys. B **6**, 3909 (1992).

[9] K.-D. Tsuei and P. D. Johnson, Solid State Commun. **101**, 337 (1997).

[10] K.-D. Tsuei, J.-Y. Yuh, C.-T. Tzeng, R.-Y. Chu, S.-C. Chung, and K.-L. Tsang, Phys. Rev. B **56**, 15 412 (1997).

[11] G. K. Wertheim and D. N. E. Buchanan, Phys. Rev. B **50**, 11 070 (1994).

[12] L. H. Tjeng, R. Hesper, A. C. L. Heessels, A. Heeres, H. T. Jonkman, and G. A. Sawazky, Solid State Commun. **103**, 31 (1997).

[13] R. Hesper, L. H. Tjeng, and G. A. Sawazky, Europhys. Lett. **40**, 177 (1997).

[14] J. Kovac, G. Scarel, O. Sakho, and M. Sancrotti, J. Electron Spectrosc. Relat. Phenom. **76**, 405 (1995).

[15] E. Magnano, S. Vandre, C. Cepek, A. Goldoni, A. D. Laine, G. M. Curro, A. Santaniello, and M. Sancrotti, Surf. Sci. **377–379**, 1066 (1997).

[16] M. R. C. Hunt, S. Modesti, P. Rudolf, and R. E. Palmer, Phys. Rev. B **51**, 10 039 (1995).

[17] C. Cepek, A. Goldoni, and S. Modesti, Phys. Rev. B **53**, 7466 (1996).

[18] M. W. Ruckman, B. Xia, and S. L. Qiu, Phys. Rev. B **48**, 15 457 (1993).

[19] G. K. Wertheim and D. N. E. Buchanan, Solid State Commun. **88**, 97 (1993).

[20] S. C. Wu, K. Xun, J. Z. Deng, J. Yao, F. Q. Liu, S. H. Lea, Z. Q. Wang, R. S. Han, and Z. N. Gu, Phys. Rev. B **47**, 13 830 (1993).

[21] A. Sellidj and B. E. Koel, J. Phys. Chem. **97**, 10 076 (1993); L. Q. Jiang and B. E. Koel, Phys. Rev. Lett. **72**, 140 (1993).

[22] A. V. Hamza, J. Dykes, W. D. Mosley, L. Dinh, and M. Balooch, Surf. Sci. **318**, 368 (1994).

[23] A. J. Maxwell, P. A. Bruhwiler, S. Andersson, D. Arvantis, B. Hernnas, O. Karis, D. C. Mancini, N. Martensson, S. M. Gray, M. K.-J. Johansson, and L. S. O. Johansson, Phys. Rev. B **52**, R5546 (1995).

[24] A. J. Maxwell, P. A. Bruhwiler, D. Arvantis, J. Hasselstrom, and N. Martensson, Phys. Rev. Lett. **79**, 1567 (1997).

[25] A. J. Maxwell, P. A. Bruhwiler, D. Arvantis, J. Hasselstrom, M. K.-J. Johansson, and N. Martensson, Phys. Rev. B **57**, 7312 (1998).

[26] A. F. Hebard, M. J. Rosseinsky, R. C. Haddon, D. W. Murphy, S. J. Duclos, K. B. Lyons, B. Miller, J. M. Rosamilia, R. M. Fleming, A. R. Kortan, S. H. Glarum, A. V. Makhija, A. J. Muller, R. H. Eick, S. M. Zahurak, R. Tycko, G. Dabbagh, and F. A. Thiel, Nature (London) **350**, 600 (1991).

[27] K. Tanigaki, T. W. Ebbesen, S. Saito, J. Mizuki, J. S. Tsai, Y. Kubo, and S. Kuroshima, Nature (London) **352**, 222 (1991).

[28] P. J. Benning, D. M. Poirier, T. R. Ohno, Y. Chen, M. B. Jost, F. Stepniak, G. H. Kroll, J. H. Weaver, J. Fure, and R. E. Smalley, Phys. Rev. B **45**, 6899 (1992).

[29] T. Kobayashi, C. Tindall, O. Takaoka, Y. Hasegawa, and T. Sakurai, J. Korean Phys. Soc. **31**, S5 (1997).

[30] C. T. Chen, L. H. Tjeng, P. Rudolf, G. Meigs, J. E. Rowe, J. Chen, J. P. McCauley, Jr., A. B. Smith III, A. R. McGhie, W. J. Romanow, and E. W. Plummer, Nature (London) **352**, 603 (1991).

[31] K. Motai, T. Hashizume, H. Shinohara, Y. Saito, H. Pickering, Y. Nishina, and T. Sakurai, Jpn. J. Appl. Phys. **32**, L450 (1993); T. Hashizume, K. Motai, X. D. Wang, H. Shinohara, Y. Saito, Y. Maruyama, K. Ohno, Y. Kawazoe, Y. Nishina, H. Pickering, Y. Kuk, and T. Sakurai, Phys. Rev. Lett. **71**, 2959 (1993).

[32] E. Altman and R. Colton, Surf. Sci. **279**, 49 (1992); **295**, 13 (1993).

[33] E. Altman and R. Colton, Phys. Rev. B **48**, 18 244 (1993).

[34] T. David, J. K. Gimzewski, D. Purdie, B. Reihl, and R. R. Schlittler, Phys. Rev. B **50**, 5810 (1994); J. K. Gimzewski, S. Modesti, T. David, and R. R. Schlittler, J. Vac. Sci. Technol. B **12**, 1942 (1994).

[35] J. K. Gimzewski, S. Modesti, and R. Schlittler, Phys. Rev. Lett. **72**, 1036 (1994); S. Modesti, J. K. Gimzewski, and R. Schlittler, Surf. Sci. **331–333**, 1129 (1995).

[36] Y. Kuk, D. K. Kim, Y. D. Suh, K. H. Park, H. P. Noh, S. J. Oh, and S. K. Kim, Phys. Rev. Lett. **70**, 1948 (1993).

[37] Many STM studies of fullerenes on both metal and semiconductor surfaces can be found in the review article by T. Sakurai, X.-D. Wang, Q. K. Xue, Y. Hasegawa, T. Hashizume, and H. Shinohara, Prog. Surf. Sci. **51**, 263 (1996).

[38] M. K.-J. Johansson, A. J. Maxwell, S. M. Gray, P. A. Bruhwiler, D. C. Mancini, and N. Martensson, Phys. Rev. B **54**, 13 472 (1996); M. K.-J. Johansson, A. J. Maxwell, S. M. Gray, P. A. Bruhwiler, and L. S. O. Johansson, Surf. Sci. **397**, 314 (1998).

[39] J. H. Weaver and D. M. Poirier, in *Solid State Physics*, edited by H. Ehrenrich and F. Spaepen (Academic, Boston, 1994), Vol. 48, p. 1.

[40] A. Fartash, Appl. Phys. Lett. **67**, 3901 (1995); Phys. Rev. B **52**, 7883 (1995).

[41] S. D. Kevan and R. H. Gaylord, Phys. Rev. B **36**, 5809 (1987).

[42] R. C. Haddon, L. E. Brus, and K. Raghvachari, Chem. Phys. Lett. **125**, 459 (1985).

[43] P. J. Benning, D. M. Poirier, N. Troullier, J. L. Martins, J. H. Weaver, R. E. Haufler, L. P. F. Chibante, and R. E. Smalley, Phys. Rev. B **44**, 1962 (1991).

[44] We used a similar analysis to estimate the Fermi-level crossing of C_{60}/Cu(111) in Ref. 10. It gives 1.6 electrons per molecule, consistent with other analyses.

[45] J. Wu, Z.-X. Shen, D. S. Dessau, R. Cao, D. S. Marshall, P. Pianetta, I. Lindau, X. Yang, J. Terry, D. M. King, B. O. Wells,

D. Elloway, H. R. Wendt, C. A. Brown, H. Hunziker, and M. S. de Vries, Physica C **197**, 251 (1992).

[46] T. Liebsch, O. Plotzke, F. Heiser, U. Hergenhahn, O. Hemmers, R. Wehlitz, J. Viefhaus, B. Langer, S. B. Whitfield, and U. Becker, Phys. Rev. A **52**, 457 (1995).

[47] Y. B. Xu, M. Q. Tan, and U. Beker, Phys. Rev. Lett. **76**, 3538 (1996).

[48] J. H. Weaver, J. L. Martins, T. Komeda, Y. Chen, T. R. Ohno, G. H. Kroll, N. Troullier, R. H. Haufler, and R. E. Smalley, Phys. Rev. Lett. **66**, 1741 (1991); P. J. Benning, D. M. Poirier, T. R. Ohno, Y. Chen, M. B. Jost, F. Stepniak, J. Fure, and R. E. Smalley, Phys. Rev. B **45**, 6899 (1992); S. Krummacher, M. Biermann, M. Neeb, A. Liebsch, and W. Eberhardt, *ibid.* **48**, 8424 (1993).

[49] C. Enkvist, S. Lunell, B. Sjogren, S. Svensson, P. A. Bruhwiler, A. Nilsson, A. Maxwell, and N. Martensson, Phys. Rev. B **48**, 14 629 (1993).

[50] M. B. Jost, N. Troullier, D. M. Poirier, J. L. Martins, J. H. Weaver, L. P. F. Chibante, and R. E. Smalley, Phys. Rev. B **44**, 1966 (1991).

[51] D. A. King, Surf. Sci. **47**, 384 (1975).

[52] A. Tokmakoff, D. R. Haynes, and S. M. George, Chem. Phys. Lett. **186**, 450 (1991).

[53] A. V. Hamza and M. Balooch, Chem. Phys. Lett. **198**, 603 (1992).

[54] C. Kittel, *Introduction to Solid State Physics*, 5th ed. (Wiley, New York, 1976), p. 83.

[55] R. Luthi, E. Meyer, H. Haefke, L. Howald, W. Gutmannsbauer, and H.-J. Guntherodt, Science **266**, 1979 (1994).

[56] *CRC Handbook of Chemistry and Physics*, 75th ed. (CRC Press, Boca Raton, FL, 1995).

[57] K.-D. Tsuei, C.-T. Tzeng, J.-Y. Yuh, and S.-C. Chung (unpublished).

[58] D. A. Papaconstantopoulos, *Handbook of the Band Structures of Elemental Solids* (Plenum, New York, 1986).